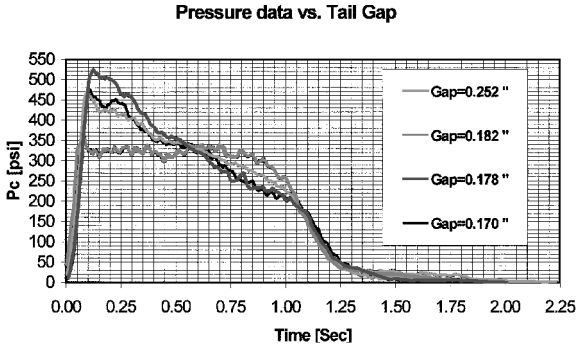

Fig. 2 Static test results of pressure histories vs the tail gap.

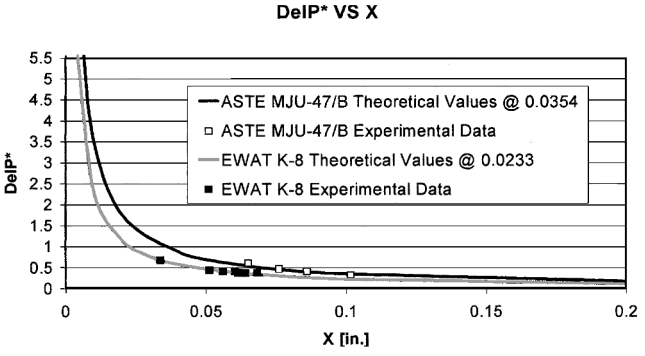

Fig. 3 Pressure ratio ΔP^* vs X: experimental vs theoretical data.

ratio, which indicates higher values of pressure spike for smaller X values). These findings show that Eq. (4) provides a reasonable prediction of the pressure spike value once the burn rate and the rise time are known.

Discussion

Variational principles[8] dictate that for equilibrium conditions to occur both sides of Eq. (2) should vanish. Keeping steady-state terms separated from the unsteady terms enables separate equilibrium conditions for each of these states. This seems not only mathematically correct but also true to the physical meaning of the substantial derivative decomposition procedure in the mass flow balance. The geometric characteristic length, which defines the ratio between the void volume and the throat area, was obtained[4] by mixing steady and unsteady terms. In contrast, the physical interpretation of the new equilibrium conditions is that, when the throat area is changed, new steady-state conditions and performance occur, and thus the stage is set for different unsteady-state equilibrium conditions. In the presented experimental tests, the throat area remained unchanged, but pressure spikes occurred (see Fig. 2) as the X changed. Furthermore, the two motors reported in this study with different port area and case diameter showed that variations in X correlated well with the pressure spike. Finally, note [Eq. (5)] that the connecting term between the purely unsteady condition, X, and the purely steady condition, K_n, is the geometric characteristic length L^*, which was originally derived from mixed terms.

Conclusions

A new design criterion for unsteady equilibrium in SRM was derived from the conservative mass balance equation in integral form. This relation [Eq. (4)] shows the dependency not only of the pressure spike on grain properties (such as burn rate and rise time) but also on a geometric parameter called the characteristic gap. The characteristic gap X defines the ratio between the void volume and the propellant burning surface. In basic motor design, it is sometimes close in dimension to the physical gap between the throat and the end-grain surface. The new unsteady-state equilibrium was corroborated with the experimental data and was found to work consistently as a design tool to predict pressure spikes early in the design.

More experimental testing is suggested. The correlation between the X and the pressure spike should be clearly demonstrated in an end-burning-type test apparatus. In contrast to SRMs with complex grain geometry, end-burning-type test setups will enable visual verification of the relationship between the SRM geometric parameters and the design criteria of equilibrium conditions.

Acknowledgment

The research reported in this Note was funded in part by the ASIE program, Wright–Patterson AFB, Ohio 45433-7017, Contract no. 33657-95-C-0006.

References

[1] Sutton, G. P., *Rocket Propulsion Elements*, 6th ed., Wiley, New York, 1992, Sec. 11.2, p. 384.

[2] Zucrow, M. J., *Aircraft and Missile Propulsion*, Vol. 1, Wiley, New York, 1958, pp. 91, 92.

[3] Zucrow, M. J., *Aircraft and Missile Propulsion*, Vol. 2, Wiley, New York, 1958, pp. 419–433.

[4] Barrere, M., Jaumotte, A., De Veubeke, B. F., and Vandenkerchove, J., *Rocket Propulsion*, Elsvier, New York, 1960, pp. 237–247.

[5] Hill, P. G., and Peterson, C. P., *Mechanics and Thermodynamics of Propulsion*, Addison Wesley Longman, Reading, MA, 1987, pp. 117–119.

[6] Brooks, W. T., Workshop Report: Burn Rate Determination Methodology, CPIA Publ. 347, Vol. 2, Chemical Propulsion Information Agency, Columbia, MD, Oct. 1981, pp. 183–191.

[7] Kruse, R. B., *Fundamental of Solid Rocket Motors*, Univ. of Huntsville Press, Huntsville, AL, 1991, p. 27.

[8] Yourgrau, W., and Mandelstam, S., *Variational Principles in Dynamics and Quantum Theory*, Dover, New York, 1979, Sec. 4, pp. 145–152.

Concentration Measurements in a Mixing Module for Lean, Premixed, Gas-Turbine Combustors

D. Douglas Thomsen,* R. V. Ravikrishna,†
Clayton S. Cooper,* Yanan Jiang,§
and Normand M. Laurendeau¶
Purdue University, West Lafayette, Indiana 47907-1288

Introduction

RECENT government emission standards mandating low NO_x levels in advanced gas-turbine engines have led to the use of lean, premixed combustion.[1] Lean, premixed combustion reduces thermal NO_x by preventing the creation of the high-temperature, stoichiometric interfaces found in traditional diffusion flames. However, the advantages of this technique depend upon the flame burning at the same lean equivalence ratio at all locations and times. The exponential dependence of NO_x on temperature causes relatively small spatial or temporal variations in equivalence ratio to produce substantial increases in NO_x emissions.[2] Thus, mixing efficiency is a critical property of any proposed lean-premixed combustor.

One proposed design for achieving the goal of well-mixed lean combustion for natural gas applications, while minimizing the

Received 28 February 1999; revision received 5 January 2000; accepted for publication 25 February 2000.

*Researcher; currently Combustion Design Engineer, Advanced Combustion Engineering, General Electric Aircraft Engines, Cincinnati, OH.

†Researcher; currently Assistant Professor, Department of Mechanical Engineering, Indian Institute of Science, Bangalore, India.

§Research Associate, Department of Chemistry.

¶Reilly Professor of Combustion; currently Ralph and Bettye Bailey Professor of Combustion.

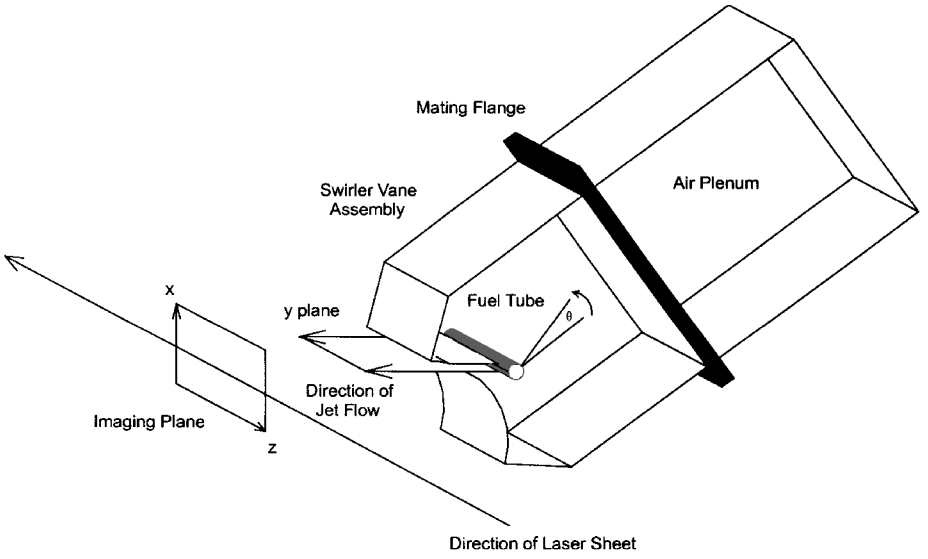

Fig. 1 Diagram of swirler-vane/fuel-tube assembly showing coordinate system used for this study. The distance from the fuel tube to the far edge of the assembly, along the *y* axis, is ~ 25 mm.

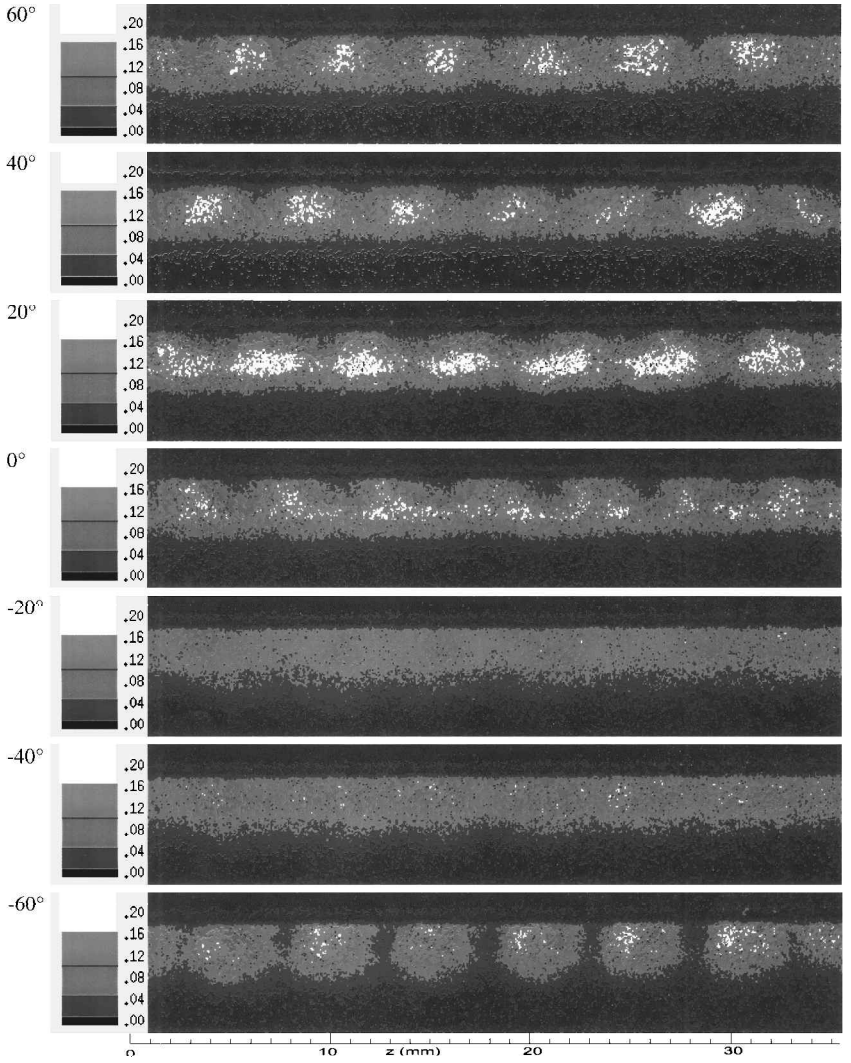

Fig. 2 PLIF images of fuel mole fraction as a function of fuel-tube angle for the first fuel-tube configuration. Images taken ~ 17 mm from the center of the fuel tube. Color-coded bar to right of image represents fuel mole fraction.

danger of flashback and instability, is the lean premix module developed by Rolls-Royce/Allison.[3] This module consists of 16 fuel delivery tubes located between air swirl vanes at the entrance to a radial-inflow swirler. Each delivery tube has holes placed along its length for fuel injection. Locating and sizing the fuel-injection holes to optimize the mixing within each swirler-vane/fuel-tube assembly is vital to obtaining short premixers. Hence, experimental measurements of fuel concentration at the swirler-vane exit are needed to validate the utility of the current design.

Acetone laser-induced fluorescence (LIF) is one technique that has recently been used as a tracer for concentration measurements in gaseous flows.[4–6] As a laser-based technique, it does not disrupt the flowfield. Moreover, acetone has a fairly broad ultraviolet absorption spectrum and a spectrally isolated, although broad, visible fluorescence spectrum. In addition, acetone's high volatility makes it easy to vaporize so as to obtain large concentrations in a simulated gaseous fuel stream.

This Note reports on acetone planar LIF (PLIF) measurements of average fuel concentration at the exit plane of a swirler-vane/fuel-tube assembly corresponding to the Rolls-Royce/Allison Radial Swirler Plus Nozzle lean premix module. These measurements are used to identify regions of spatial unmixedness and to study the effect of fuel-tube configuration on this unmixedness. The project was designed to utilize simple, mean measurements in an effort to quickly identify design corrections in the experimental assembly.

Experimental Methods

The UV-excitation spectrum of acetone is fairly broad [~100 nm full width at half-maximum (FWHM)] and is centered at approximately 275 nm (Ref. 4). For this work the excitation wavelength is generated by employing the second harmonic ($\lambda = 532$ nm) of a Quanta-Ray DCR-3G Nd:YAG laser to pump a Molectron DL-II dye laser. The resulting beam produced by the Rhodamine 590 dye is then frequency doubled to obtain the desired excitation wavelength of 280 nm (10-ns FWHM, 6 mJ/pulse). The excitation beam was focused using a 1000-mm focal length lens coupled with a cylindrical lens to vertically expand and collimate the excitation beam. An aperture/slit assembly, positioned immediately before the swirler-vane/fuel-tube assembly, was used to clip the wings of the sheet (~10 mm tall × 200 μm wide). A wideband interference filter spectrally centered at 465 nm and having an 80-nm FWHM was used to reject laser scattering at 280 and 532 nm while retaining the linear acetone fluorescence. The spectrally filtered PLIF image was spatially amplified, discretized, and registered using a 12-bit Princeton Instruments ICCD detector (Princeton Instruments ST-130), which incorporated a 578 × 384 pixel charge-coupled device. Typically, 150 fluorescence events were integrated on chip for each image, with

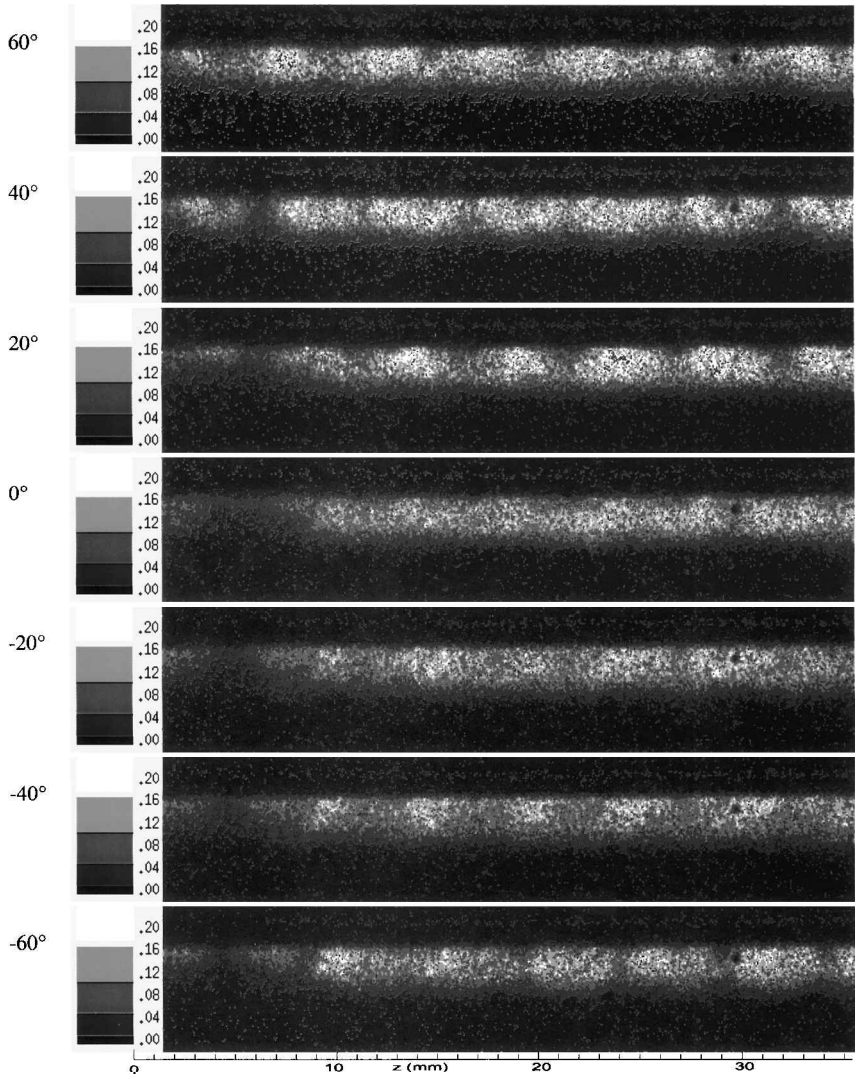

Fig. 3 PLIF images of fuel mole fraction as a function of fuel-tube angle for the second fuel-tube configuration. Images taken ~17 mm from the center of the fuel tube. Color-coded bar to right of image represents fuel mole fraction.

each event gated over an ~30-ns period. Image analysis and reduction were performed on a laboratory Sparc station using PV-WAVE v.6.01 software (Visual Numerics, Inc.).

Calibration was performed by flowing a gas stream of known acetone concentration through a tube and obtaining an image of the acetone fluorescence in the resulting jet. The average value of this fluorescence signal, which represented a fuel mole fraction of unity, was determined over a region in the center of the jet. The fluorescence image of the flow from the swirler-vane/fuel-tube assembly was normalized by this value so as to yield an image displaying fuel mole fraction. Nonuniformities in the laser sheet were accounted for by recording a Rayleigh scattering image of the laser sheet, which was then used to normalize both the calibration and the fluorescence image.

A diagram of the swirler-vane/fuel-tube assembly is shown in Fig. 1 along with the coordinate system used for this study. The x coordinate is perpendicular to both the airflow and the fuel tube, as measured from the centerline of the fuel tube. The y coordinate is the distance along the airflow measured from the centerline of the fuel tube. The z coordinate is parallel to the fuel tube. The angle θ represents tube rotation about the z axis with positive rotations being counterclockwise for the view shown in Fig. 1. The reference angle for θ is the angle at which the perpendicular bisector between the two rows of fuel injection holes passes through the midpoint of the lean premix module. Two different fuel-tube configurations were studied in the current work. The first had two rows of fuel-injection holes, one with seven and the other with eight equally spaced holes, offset from each other and separated by an included angle of 90 deg. The second configuration differed only in the included angle that was modified to be 120 deg. To match the molecular weight of CH_4, the fuel stream consisted of one standard liters per minute (SLPM) of N_2 bubbled through 35°C acetone, as maintained by a temperature-controlled water bath, followed by dilution with an additional 5.07 SLPM of N_2 and 9.05 SLPM of He, for a combined flow rate of 15.97 SLPM and an acetone mole fraction of 0.00266. These flow rates correspond to an overall equivalence ratio of 0.5 when used with the desired airflow rate of 6 g/s (304 SLPM) and yield roughly equal fuel and air velocities at the location of fuel injection (~30 m/s).

PLIF Measurements

PLIF images of fuel mole fraction were obtained perpendicular to the main airflow. Each PLIF image represents a specific distance y from the center of the fuel tube. The primary goal of this study was to determine the orientation angle θ, which optimizes the temporally averaged mixing efficiency for each of two fuel-tube configurations supplied by Rolls-Royce/Allison, and to determine the sensitivity of the average mixing efficiency to small changes in θ. Starting with the first fuel-tube configuration, Fig. 2 shows the effect of tube rotation on fuel concentration at the exit of the swirler-vane/fuel-tube

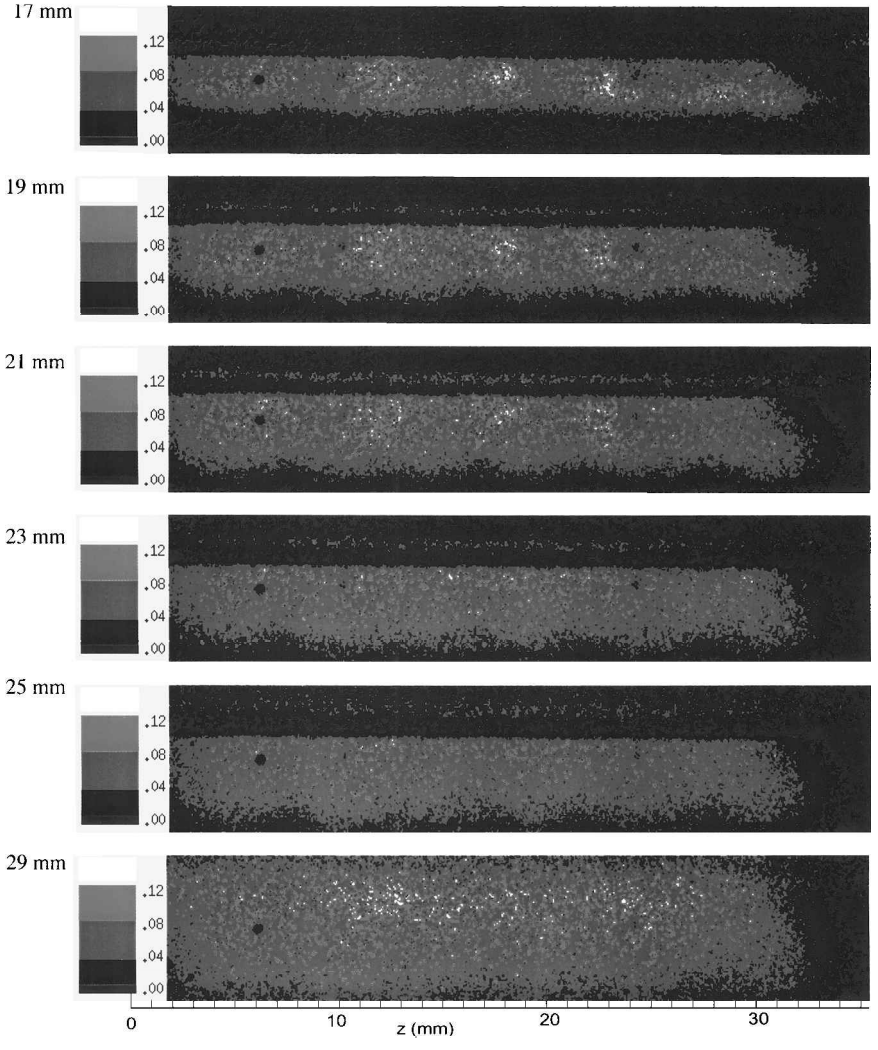

Fig. 4 PLIF images of fuel mole fraction as a function of distance from the fuel tube for the second fuel-tube configuration (θ = 0 deg). Color-coded bar to right of image represents fuel mole fraction.

assembly ($y \approx 17$ mm). Figure 2 indicates that significant average unmixedness exists at the exit plane of the assembly for the reference angle $\theta = 0$ deg. The images also demonstrate that small positive changes in θ tend to further degrade the mixing efficiency of this assembly. However, a small negative rotation to an orientation of $\theta = -20$ deg results in a much more uniform fuel distribution across the fuel/air jet.

Similar results are shown for the second fuel-tube configuration in Fig. 3. As compared to the first fuel-tube configuration, this module displays improved mixing efficiency at its base reference angle. In response to changes in θ, positive rotation of the fuel tube once again decreases the mixedness of the fuel-airflow. However, for this case the base orientation, rather than a slightly negative fuel-tube angle, seems to provide optimal mixing. The implication is that fuel-jet mixing occurs primarily via crossflow of preswirler air over the fuel tube. As shown by Fig. 3, the second configuration has the additional benefit of being less sensitive to small changes in fuel-tube angle.

Finally, we determined how rapidly mixing occurred within the fuel-air stream as a function of downstream distance. Because these fuel/air streams enter into a larger swirler assembly prior to combustion, unmixedness at the exit of the swirler-vane/fuel-tube assembly is only a problem if it persists into the reaction zone. Figure 4 shows fuel-concentration distribution as a function of distance from the fuel tube, along the fuel-air jet, for the second fuel-tube configuration ($\theta = 0$ deg). Although a fair amount of unmixedness occurs at the exit plane (17 mm), nearly complete fuel-air mixing occurs at $\sim$23 mm from the fuel-tube centerline and well before the end of the swirler-vane module. In fact, at this location the average fuel mole fraction is 0.083 as compared to the fully mixed mole fraction of 0.05.

Conclusion

In conclusion, simple qualitative measurements of the type presented in this study can be crucial to optimization of fuel-air mixedness and thus minimization of NO_x emissions from lean premixed combustors. Additional parameters such as fuel type, fuel/air momentum ratio, or air preheat temperature can be effectively studied on both a spatial- and time-averaged basis via acetone PLIF measurements of surrogate fuel.

Acknowledgments

This work was supported by a contract from Rolls-Royce/Allison (Indianapolis, IN), with Mohan Razdan as research monitor. The authors would like to acknowledge Steve Frey at Rolls-Royce/Allison for his design and development of the swirler-vane/fuel-tube assemblies used in this investigation.

References

[1]Correa, S. M., "Power Generation and Aeropropulsion Gas Turbines: from Combustion Science to Combustion Technology," *Proceedings of the Twenty-Seventh International Symposium on Combustion*, Combustion Inst., Pittsburgh, PA, 1998, pp. 1793–1807.

[2]Fric, T. F., "Effects of Fuel-Air Unmixedness on NO_x Emissions," *Journal of Propulsion and Power*, Vol. 9, No. 5, 1993, pp. 708–713.

[3]Puri, R., Stansel, D. M., Smith, D. A., and Razdan, M. K., "Dry Ultralow NO_x "Green Thumb" Combustor for Allison's 501-K Series Industrial Engines," *Journal of Engineering for Gas Turbines and Power*, Vol. 119, No. 1, 1997, pp. 93–101.

[4]Lozano, A., Yip, B., and Hanson, R. K., "Acetone: a Tracer for Concentration Measurements in Gaseous Flows by Planar Laser-Induced Fluorescence," *Experiments in Fluids*, Vol. 13, No. 6, 1992, pp. 369–376.

[5]Lozano, A., Smith, S. H., Mungal, M. G., and Hanson, R. K., "Concentration Measurements in a Transverse Jet by Planar Laser-Induced Fluorescence of Acetone," *AIAA Journal*, Vol. 32, No. 1, 1993, pp. 218–221.

[6]Frazier, T. R., Foglesong, R. E., Coverdill, R. E., Peters, J. E., and Lucht, R. P., "An Experimental Investigation of Fuel/Air Mixing in an Optically Accessible Axial Premixer," AIAA Paper 98-3543, July 1998.

Radiation and NO_x Pathways in Nonpremixed Turbulent Flames

D. Lentini*
University of Rome "La Sapienza," I–00184 Rome, Italy
and
I. K. Puri†
University of Illinois at Chicago, Chicago, Illinois 60607-7022

Introduction

CURRENT demanding standards require accurate predictions of NO_x outflow from flames and combustors. Turbulent flows hamper a detailed accounting of NO_x formation; the standard approach considers only the thermal pathway in adiabatic conditions. However, NO_x formation involves different pathways[1]: thermal, nitrous oxide, prompt, nitric dioxide, and fuel.

This investigation introduces a treatment for heat losses by radiation in optically thin nonsooting flames and explores the reaction regimes of the various NO_x pathways. The model is based on the stretched laminar flamelet (SLF) approach, which considers a turbulent flame to consist of thin laminar flamelets. Chemical processes characterized by a timescale shorter than the Kolmogorov time t_K contribute to the definition of their structure, whereas those involving a timescale larger than t_K occur in the distributed reaction regime; a finer division discriminates between the regions $t_K < t_c < t_I$ and $t_c > t_I$, where t_I is the integral scale. Provided that the processes are energetically insignificant (as in the case of NO_x) and uncoupled from faster paths a treatment can be devised for the latter regime as well.

Central to the SLF approach is the identification of the characteristic chemical time of the different NO_x pathways. This paper defines the elements required to investigate the reaction regime of the thermal and N_2O pathways.

Treatment of Heat Loss Effects via the SLF Approach

An extension of the SLF formalism to nonadiabatic combustion, as suggested in Ref. 2, has recently been developed.[3] It is based on the introduction of an enthalpy defect given in the following equation, in addition to the conserved scalar (or mixture fraction, defined in terms of enthalpy) Z and the scalar dissipation rate χ_c (conditioned at the flame front):

$$\zeta = h - [h_o + Z(h_f - h_o)] \tag{1}$$

that is, the gap between the actual enthalpy and that of an adiabatic flame (h_o, h_f refer to oxidizer and fuel). State quantities in laminar flames can then be expressed as

$$\phi = \phi(Z; \chi_c; \zeta) \tag{2}$$

so that average values can be recovered by convolution with an appropriately defined joint probability density function (PDF) of Z, χ_c, and ζ. The approach requires an additional equation for $\tilde{h}$, to recover $\tilde{\zeta}$ after averaging the linear relationship (1). The SLF model for turbulent flames requires as an input a library of laminar flames, with properties expressed in form (2). Profiles must be organized in shelves, where each shelf contains entries for numerous χ_c values from equilibrium to extinction plus the inert (or pure-mixing) state, and each shelf refers to a different value of ζ.

Received 20 December 1997; revision received 29 October 1999; accepted for publication 9 December 1999.

*Associate Professor, Department of Mechanics and Aeronautics, Via Eudossiana 18.

†Professor, Mail Code 251, Department of Mechanical Engineering, 842 W. Taylor Street.